Solution Structures of 5-Fluorouracil-Substituted DNA and RNA Decamer Duplexes†

Parag V. Sahasrabudhe,‡ Richard T. Pon,§ and William H. Gmeiner*,‡

Eppley Cancer Institute and Department of Pharmaceutical Sciences, University of Nebraska Medical Center, Omaha, Nebraska 68198-6805, and Regional DNA Synthesis Laboratory, University of Calgary, Calgary, Alberta T2N 4N1, Canada

Received March 4, 1996; Revised Manuscript Received August 6, 1996⊗

ABSTRACT: The structures in solution of eight oligonucleotide duplexes each containing either zero, one, or two 5-fluorodeoxyuridine (FdUrd) or 5-fluorouridine (FUrd) nucleosides were determined by the combined use of NMR spectroscopy, restrained molecular dynamics, and full relaxation matrix refinement to determine how FdUrd and FUrd substitution affects the structure of duplex DNA and RNA and to establish whether structural differences due to FdUrd and FUrd substitution in nucleic acids may be responsible, in part, for the biological effects of the anticancer drug 5-fluorouracil (FUra). The nucleic acid directed effects of FUra include induction of single-strand breaks in duplex DNA and altered processing of pre-mRNA and rRNA. Four self-complementary oligodeoxyribonucleotide sequences were prepared and studied as duplexes in aqueous solution: (5′ dGCGAAUUCGC)$_2$, (5′ dGCGAAUFCGC)$_2$, (5′ dGCGAAFUCGC)$_2$, and (5′ dGCGAAFFCGC)$_2$. The corresponding oligoribonucleotide sequences (5′ rGCGAAUUCGC)$_2$, (5′ rGCGAAUFCGC)$_2$, (5′ rGCGAAFUCGC)$_2$, and (5′ rGCGAAFFCGC)$_2$ were also prepared and studied. The helical parameters for the structures of these eight duplexes were analyzed to determine how substitution of FdUrd and FUrd affects the three-dimensional structures of duplex DNA and RNA. FdUrd substitution affects the base roll angle at the site of FdUrd substitution, causing the helical axis of FdUrd-substituted DNA duplexes to be bent compared to the nonsubstituted duplex. A-FUrd base pairs show substantial RMS deviations from A-Urd base pairs in all three of the RNA duplexes substituted with FUrd. Bending of the helical axis due to FdUrd substitution may contribute to the occurrence of single-strand breaks in duplex DNA while the altered structures of A-FUrd base pairs may affect RNA−RNA and RNA−protein recognition.

The nucleoside antimetabolite 5-fluorouracil (FUra)[1] is the principal chemotherapeutic agent used clinically in the treatment of solid tumors, particularly for gastrointestinal malignancies (Pratt *et al.*, 1994). The anticancer activity of FUra is believed to result primarily from its metabolism to FdUMP and the inhibition of dTMP production (Weckbecker, 1991). FdUMP, together with 5,10-methylenetetrahydrofolate, forms an extremely stable ternary complex with thymidylate synthase, the enzyme required for dTMP production and DNA replication (Santi *et al.*, 1974). FUra may also exert anticancer and cytotoxic activities as a consequence of its metabolism to FUTP and the incorporation of FUrd into cellular RNA (Doong & Dolnick, 1988) and also by the incorporation of FdUTP into genomic DNA that can result in single- and double-strand breaks. The effects of FUra metabolites on RNA and DNA biochemistry are collectively referred to as the RNA- and DNA-mediated effects of FUra. It is not known whether direct conformational effects that result from FdUrd and FUrd substitution in DNA and RNA are important for the cytotoxic and anticancer activity of FUra. In the present work, the effects of FdUrd and FUrd substitution on the structures of duplex DNA and RNA are systematically evaluated to better understand how substitution of FUra metabolites in nucleic acids may be responsible, in part, for the biological activity of FUra.

The relationship between the incorporation of FdUrd into genomic DNA and the cytotoxic and anticancer activities of fluorinated pyrimidines is not known. FdUrd incorporation into duplex DNA may lead to base pair mismatches during transcription that result in the synthesis of mutant, dysfunctional proteins. FdUrd substitution could also affect the recognition of duplex DNA by transcription factor complexes and interfere with gene regulation. NMR spectroscopic studies of oligodeoxyribonucleotide duplexes have revealed that the rate of base pair opening for an dA-FdUrd base pair is greater than for an dA-dT base pair (Sowers *et al.*, 1987) whereas dG-FdUrd base pairs engage in an equilibrium between wobble base pair geometry and an ionized base pair (Sowers *et al.*, 1988). The ionization of FdUrd stimulates base mispairing frequencies with dG (Yu *et al.*, 1993). X-ray crystallographic studies of FdUrd-substituted Z-DNA indicate that substitution results in little distortion to this form of DNA (Coll *et al.*, 1989). The biological significance of base pair mismatches involving FdUrd in DNA−DNA and DNA−

† This research was supported by funds from NIH-NCI R29CA60612 (W.H.G.) and NIH-NCI CA36727.

* Address correspondence to this author. Fax: (402) 559-4651. Phone: (402) 559-4257. E-mail: bgmeiner@unmc.edu.

‡ University of Nebraska Medical Center.

§ University of Calgary.

⊗ Abstract published in *Advance ACS Abstracts,* October 1, 1996.

[1] Abbreviations: FUra, 5-fluorouracil; FUrd, 5-fluorouridine; FdUrd, 5-fluoro-2′-deoxyuridine; FdUMP, 5-fluoro-2′-deoxyuridine monophosphate; FdUTP, 5-fluoro-2′-deoxyuridine triphosphate; FUTP, 5-fluorouridine triphosphate; dTMP, thymidine triphosphate; dG, 2′-deoxyguanosine; dA, 2′-deoxyadenosine; dT, thymidine; dUrd, 2′-deoxyuridine.

S0006-2960(96)00535-1 CCC: $12.00

RNA duplexes is unclear since accumulation of FdUrd into DNA is slight and incorporation of FdUrd into genomic DNA tends to parallel the magnitude of the other biological effects of FUra (Pratt *et al.*, 1994).

Although much of the anticancer activity of FUra can be explained by thymidylate synthase inhibition and DNA strand breaks, the metabolic conversion of FUra to FUTP and the subsequent disruption of RNA-mediated processes by RNA substituted with FUra are also believed to account for some of the anticancer and cytotoxic behavior of FUra (Weckbecker, 1991). Evidence for the importance of the so-called RNA-mediated biological effects of FUra include the observation of cytotoxicity of FUra toward cells given dT exogenously (Spiegelman *et al.*, 1980), the relationship between FUra incorporation rates into RNA from tumors and their response to the drug (Matsuoka *et al.*, 1992), and the observation of biological (Doong & Dolnick, 1988) and structural effects (Armstrong *et al.*, 1986) on RNA processing in cells treated with FUra. The two RNA-mediated processes believed to be most affected by FUrd substitution are rRNA assembly and pre-mRNA splicing. Conversely, the translation of mRNA is unaffected by FUrd substitution (Schmittgen *et al.*, 1994).

The solution structure of the *Eco*RI octamer restriction fragment substituted with FdUrd obtained by NMR spectroscopic analysis of synthetic oligodeoxyribonucleotides has been reported (Stolarski *et al.*, 1992). The authors compared the final, time-averaged solution structure for the FdUrd substituted oligodeoxyribonucleotide duplex obtained from restrained molecular dynamics simulations guided by constraints from NMR data to structures of similar sequences that were obtained by different methods. FdUrd-substitution affected the local structure of the DNA duplex near the site of substitution, but otherwise had little structural effect. Detailed structural analyses describing the effects of the substitution of FUrd for Urd on the structure of duplex RNA have not been previously reported. Additional structural information on DNA and RNA substituted with FdUrd and FUrd is essential to elucidating the mechanisms of interference by fluorinated pyrimidines in nucleic acid-mediated processes.

The present study elucidates the time-averaged three-dimensional structures of four oligodeoxyribonucleotide duplexes and four oligoribonucleotide duplexes, each of which differs in the location and number of FdUrd or FUrd substitutions, but are otherwise identical. The three-dimensional time-averaged structures for these DNA and RNA duplexes were obtained by methods similar to those used to obtain the structure of the *Eco*RI DNA octamer duplex containing FdUrd by Stolarski *et al.* The parent sequence is the self-complementary decamer 5′ d/r GCGAAUUCGC. The FdUrd (FUrd) substituted duplexes have either of the two nonequivalent dUrd (Urd) residues substituted with FdUrd (FUrd) or both of these residues substituted with FdUrd (FUrd) (Figure 1). The dUrd residues were included in the DNA sequences rather than dT to facilitate comparison of these duplex DNA structures to the structures of duplex RNA of similar sequence. The value of the present study stems from the elucidation of four closely related DNA structures and four RNA structures obtained by identical methods that differ only by FdUrd (FUrd) substitution. In this manner, structural effects due to FdUrd (FUrd) substitution may be readily distinguished from other sequence-specific structural effects or effects that result from the application of different methods for structure determination. The structures obtained reveal that FdUrd substitution in duplex DNA mainly affects the helical parameter roll and causes a bending of the helical axis for the DNA duplexes substituted with FdUrd relative to the unsubstituted control. FUrd substitution in duplex RNA results in substantially greater RMS deviations for the FUrd-substituted base pairs than at other sites. These structural alterations at FUrd-A base pairs may affect RNA−RNA and RNA−protein recognition. The studies are consistent with alterations to nucleic acid structure being responsible, in part, for the nucleic acid mediated effects of FUra.

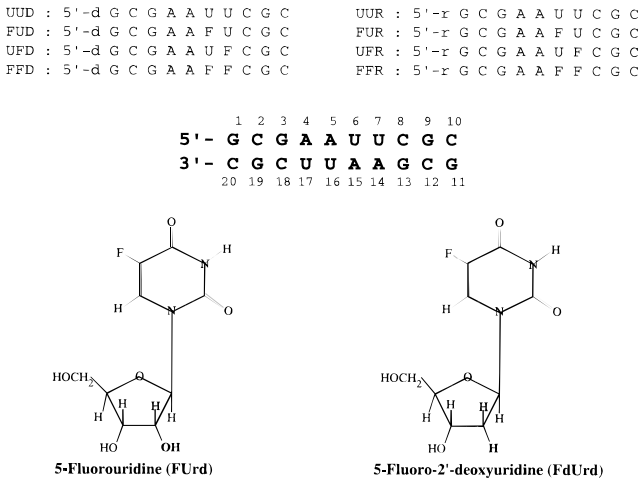

FIGURE 1: Sequences for the four self-complementary DNA duplexes [UUD], [UFD], [FUD], and [FFD] and the four self-complementary RNA duplexes [UUR], [UFR], [FUR], and [FFR] analyzed by NMR spectroscopy and rMD simulations. The numbering of individual nucleosides in the duplexes is shown for [UUD]. The structures of the monomeric nucleosides 5-fluorouridine and 5-fluorodeoxyuridine are also shown.

MATERIALS AND METHODS

Sample Preparation. The synthesis of 5′-*O*-(4,4′-dimethoxytrityl)-2′-*O*-(*tert*-butyldimethylsilyl)-5-fluorouridine 3′-(2-cyanoethyl *N*,*N*′-diisopropyl-phosphoramidite) and purification of RNA containing FUrd were done as previously described (Gmeiner *et al.*, 1994). Syntheses were performed on an Applied Biosystems 380B DNA synthesizer on a 10 μmol scale. The RNA sequences synthesized are shown in Figure 1. The preparation and purification of oligodeoxyribonucleotides containing FdUrd were accomplished essentially as described previously (Stolarski *et al.*, 1992), and the DNA sequences synthesized are also shown in Figure 1. Samples for NMR analysis in H_2O consisted of approximately 90 absorbance units (about 3 mg) of the decamer in 0.7 mL of 2 mM sodium cacodylate, pH 7.3, 100 mM NaCl, and 0.2 mM Na_2EDTA. Samples were annealed by heating to 80 °C followed by gentle cooling. The final concentrations of the oligonucleotides were approximately 1.5 mM.

NMR Measurements. All NMR experiments were performed using a Varian UNITY 500 NMR spectrometer with a 5 mm $^1H\{^{13}C,^{15}N\}$PFG probe except ^{19}F NMR spectra that were acquired using a Nalorac $^1H-^{19}F$ dual high-band probe. ^1H spectra were referenced to internal TSP (0.00 ppm) and ^{19}F spectra were referenced to external α,α,α-trifluorotoluene (0.00 ppm). One-dimensional NMR spectra in H_2O were obtained at 15 °C using a 1−3−3−1 binomial pulse for water

Table 1: Summary of Constraints Applied to Model Structures during rMD Simulations

	UUDNA	FUDNA	UFDNA	FFDNA	UURNA	FURNA	UFRNA	FFRNA
total no. of constraints	539	537	538	527	383	389	405	407
distance constraints from NMR	258	244	233	228	100	106	122	124
additional indirect constraints[a]	18	30	42	36	20	20	20	20
angle constraints from NMR	100	100	100	100	100	100	100	100
additional backbone constraints[b]								
distance	17	17	17	17	17	17	17	17
angle	94	94	94	94	94	94	94	94
hydrogen bond constraints[c]								
distance	26	26	26	26	26	26	26	26
angle	26	26	26	26	26	26	26	26

[a] Indirect loose constraints in areas poorly defined by NMR constraints (Schmitz *et al*., 1992). [b] These constraints define the right-handedness of the double helix (Baleja *et al*., 1990; Gronenborn & Clore, 1989). [c] These constraints define the Watson−Crick base pairs (Saenger, 1983).

suppression (Hore, 1989). NOESY spectra in D_2O were acquired for three different mixing times, 100, 150, and 200 ms, using the standard three-pulse sequence with States' method of phase cycling (States *et al.*, 1982). A total of 400 free induction decays (FID), 16 scans each, with alternating block acquisition, were collected in the t_1 dimension. 2K data points over a spectral width of 5000 Hz were collected in the t_2 dimension, and the carrier frequency was set at the ^{1}HDO resonance. A relaxation delay of 10 s was included between scans to allow for adequate relaxation for cross peak quantitation. All data were processed using VNMR vs 5.1 from Varian. The spectra were apodized in both dimensions using Gaussian filter functions. After zero-filling in the t_1 dimension, the final matrix was 2K × 2K real points. Baseline correction was applied to both the dimensions after the second Fourier transform. Pure absorption double-quantum-filtered COSY (DQCOSY) spectra were acquired using time-proportional phase incrementation (Marion & Wuthrich, 1983). Sixteen scans were collected for each of 800 points in the t_1 dimension, and 2K points were collected in the t_2 dimension. A square sine bell filter function, shifted by 45°, was used for apodization in both dimensions. The data matrix was 2K × 2K points after zero-filling in the t_1 dimension.

Circular Dichroism Spectra. Spectra were recorded using a Jasco J-710 spectropolarimeter. Samples were dissolved in 2 mM sodium cacodylate, pH 7.3, and 100 mM NaCl and were scanned at ambient temperature using a cylindrical cuvette with a path length of 1 mm (Sahasrabudhe *et al.*, 1995). All CD data were baseline corrected for the cell and buffer and were processed through a noise reduction program.

Calculation of Interproton Distances. Interproton distances were calculated from NOESY cross peak intensities using MARDIGRAS (Borgias & James, 1989, 1990). A complete relaxation matrix was constructed for each duplex using the experimental NOESY intensities. The experimental intensities were supplemented with intensities calculated from the model structures using CORMA (Borgias & James, 1988) to construct a complete relaxation matrix. About 280 volume integrals were evaluated for each NOESY data set, and 40 of these cross peak intensities were later rejected because they originated from overlapping cross peaks or cross peaks with low signal/noise ratio. The relaxation rates for each ^{1}H were calculated iteratively until the change in the sum of errors was minimized. Calculations were conducted for each of the eight duplexes considered in the present study (Figure 1). Calculations for each duplex were carried out with three experimental data sets (100, 150, and 200 ms mixing times), two starting geometries (energy minimized A-form and B-form), and three values for the isotropic correlation time (2, 3, and 4 ns) for a total of 18 calculations for each of the eight duplexes (144 such calculations total). Each calculation yielded estimates for upper and lower bounds for the interproton distances. The upper and lower bounds for each interproton distance from each of the 18 MARDIGRAS calculations for a given duplex were averaged, and these bounds were used for subsequent molecular dynamics simulations. Calculations for RNA duplexes differed from the calculations for DNA duplexes mainly by having fewer experimental NOESY cross peak intensities in the relaxation matrix due to lower proton density and poorer resolution for the NOESY spectra of the RNA duplexes compared to the DNA duplexes.

Simulation of DQCOSY Cross Peaks. SPHINX and LINSHA (Widmer & Wuthrich, 1987) were used to simulate DQCOSY cross peaks for the deoxyribose spin system: H1′, H2′, H2′′, H3′, H4′, and the ^{31}P spin-coupled to H3′. The cross peaks for many different sets of coupling constants and line widths were simulated. These simulated cross peaks were then compared with the experimental observations from the DQCOSY spectra. A compilation of reported values of ^{1}H−^{1}H coupling constants was used to determine the conformations of the deoxyribose rings in the DNA duplexes (Rinkel & Altona, 1987).

Construction of Molecular Models. Starting models for the oligonucleotide duplexes were built using AMBER 4.1 (Pearlman *et al.*, 1995). Each duplex was built as the canonical A-form double helix (Arnott & Hukins, 1972) and B-form double helix (Arnott & Hukins, 1973). The modified 5-fluoro-2'-deoxyuridine and 5-fluorouridine nucleosides were created using bond angles and bond lengths from a crystal structure (Harris & Macintyre,1964). Large sodium ions (hexahydrated, radius 5 Å) were added (Singh *et al.*, 1985) to mimic counterion effects. Sodium ions were placed along the PO_2^- bisection, 6 Å away from the phosphorus, and were free to move during energy minimization and molecular dynamics procedures. The starting structures were energy minimized *in vacuo* using AMBER 4.1 (Pearlman *et al.*, 1995). A combination of steepest descent and conjugate gradient methods was used.

Restrained Molecular Dynamics. The restrained molecular dynamics calculations were carried out *in vacuo* using AMBER 4.1 on an SGI Indigo workstation. Distance and angular constraints were included in the force field as pseudoenergy terms as previously described (Stolarski *et al*., 1992). The distance and torsion angle constraints applied to the model structures during rMD simulations are summarized in Table 1. The backbone dihedral angles were

constrained in a broad allowed region of the torsional angle space to preserve the right-handed character of the DNA helix during the molecular dynamics simulations (Baleja *et al.*, 1991; Gronenborn & Clore, 1989). The allowed angles were derived from a compilation of conformational angles found in different DNA types (Suzuki *et al.*, 1986). Additional distance and angular constraints were added between the bases to maintain Watson−Crick geometry during the rMD simulations (Saenger, 1983).

The rMD runs were carried out for 30 ps with 1 fs steps. All atoms within a 35 Å radius were included in nonbonded interactions. SHAKE was used to constrain all bonds (Ryckaert *et al.*, 1977), and translational and rotational motions were removed every 100 steps. The energy-minimized coordinates of A-form and B-form double helices were used as starting points. Initial velocities were taken from a Maxwellian distribution at 0.2 K. The temperature of the system was modulated during the rMD simulation as previously described (Schmitz *et al.*, 1992). The weights of the NMR and hydrogen bond constraints were modulated by multiplying the force constants by a scaling factor that varied in magnitude during the course of the rMD simulation as previously described (Schmitz *et al.*, 1992). For every rMD run of 30 ps, coordinate sets were recorded each 0.2 ps. The last 20 coordinate sets, arising from the last 4 ps of simulation, were averaged and subjected to restrained energy minimization. These simulations were run three times with different starting velocities for each run. The structure obtained from each starting model (final A-form and final B-form) resulted from averaging of the coordinates for the three structures obtained with different initial velocities. The final structure for each duplex was obtained by averaging of the two penultimate structures (final A-form and final B-form) for a particular duplex as previously described (Mujeeb *et al.*, 1993). A summary of the data obtained during the rMD simulations for each of the eight duplexes is included in the Supporting Information. The data include deviations for the distance and torsional angle restraints during the simulations, all pairwise RMS deviations for the intermediate and final structures, and energy terms for the structures obtained during the rMD simulations.

Quality of the Converged Structures. The refined structures that resulted from the rMD simulations were assessed in terms of energetics, atomic root-mean-square deviations per residue, restraint violations and the residual indices to determine the quality of the converged structures. A summary of these data is included in the Supplementary Information. The atomic RMSD values for comparing the intermediate and final structures obtained from rMD simulations to the starting A-form and B-form structures for all eight duplexes are listed in Table 2. Direct comparison of the theoretical NOESY spectrum calculated from the final structure and the experimental NOESY spectra was done using CORMA (Borgias & James, 1988). The intensities from the experimental NOESY data sets acquired with 100, 150, and 200 ms mixing times were compared to the calculated intensities for both the structures that resulted from rMD simulations and from the calculated intensities for the starting A-form and B-form structures. The results indicate that the rMD structures provide a much better fit to the experimental intensities than do the starting structures. The calculated crystallographic *R* factor and the sixth root residual R_1^x index show similar trends. These data are included in the Supporting Information.

Table 2: Comparison of RMS Deviations for the Final Structures of Eight Oligonucleotides[a]

	Final/A-final	Final/B-final	A-final/B-final
UUDNA	1.160	0.306	0.938
FUDNA	0.642	0.612	0.630
UFDNA	1.009	0.938	0.834
FFDNA	1.062	0.843	0.689
UURNA	0.331	0.530	0.470
FURNA	0.513	0.524	0.298
UFRNA	0.337	0.341	0.445
FFRNA	0.467	0.514	0.296

[a] RMS deviation between the A-form and B-form starting structures is 4.5 Å.

Structure Analysis and Display. Sugar pucker and helical parameters were calculated using the program DIALS AND WINDOWS (Ravishanker *et al.*, 1989; Lavery & Sklenar, 1988). The RMSD values between various structures were calculated using AMBER 4.1. All structures were displayed and plotted using SYBYL from TRIPOS Inc.

RESULTS

Resonance Assignments. The assignments of all the nonexchangeable protons for each of the four self-complementary DNA duplexes, [UUD], [UFD], [FUD], and [FFD] (Figure 1), were made in a sequential manner from NOESY and DQCOSY spectra in D_2O following the strategy described previously for B-form duplex DNA (Hare *et al.*, 1983; Feigon *et al.*, 1983). A portion of the NOESY spectrum for [UUD] and [UFD] showing the sequential connectivities is available as part of the Supporting Information. The adenine H2 protons were assigned by their slow relaxation rates in inversion/recovery experiments (Lee *et al.*, 1988), by the appearance of negative enhancements in 1D NOE difference spectra upon irradiation of complementary uridine imino protons (data not shown), and by the appearance of relatively weak cross peaks to H1′ of the adjacent 3′-nucleotides on the same strand in NOESY spectra. The assignments of all the nonexchangeable protons for each of the four self-complementary oligoribonucleotide duplexes, [UUR], [UFR], [FUR], and [FFR] (Figure 1), were also made in a sequential manner from NOESY and DQCOSY spectra in D_2O following the strategy described previously for A-form duplex RNA (Chou *et al.*, 1989). A portion of the NOESY spectrum for [UUR] and [UFR] showing the sequential connectivities is available as part of the Supporting Information. The adenine H2 protons were assigned as described for the DNA duplexes.

The chemical shifts of all the assigned nonexchangeable protons for [UUD] and [UUR] at 32 °C are available as part of the Supporting Information. Compilation of the base protons and H1′ for all eight DNA and RNA duplexes is also available as part of the Supporting Information. Each assigned resonance represents two protons because of the symmetry of the double helices. Differences in chemical shift for the base protons and H1′ resonances in the FdUrd (FUrd) substituted duplexes compared to the unsubstituted duplex are limited to the central four base pairs of the duplexes that contain the sites of FdUrd (FUrd) substitution. The largest differences observed are for the H6 protons of FdUrd (FUrd) residues that are shifted about 0.2 ppm

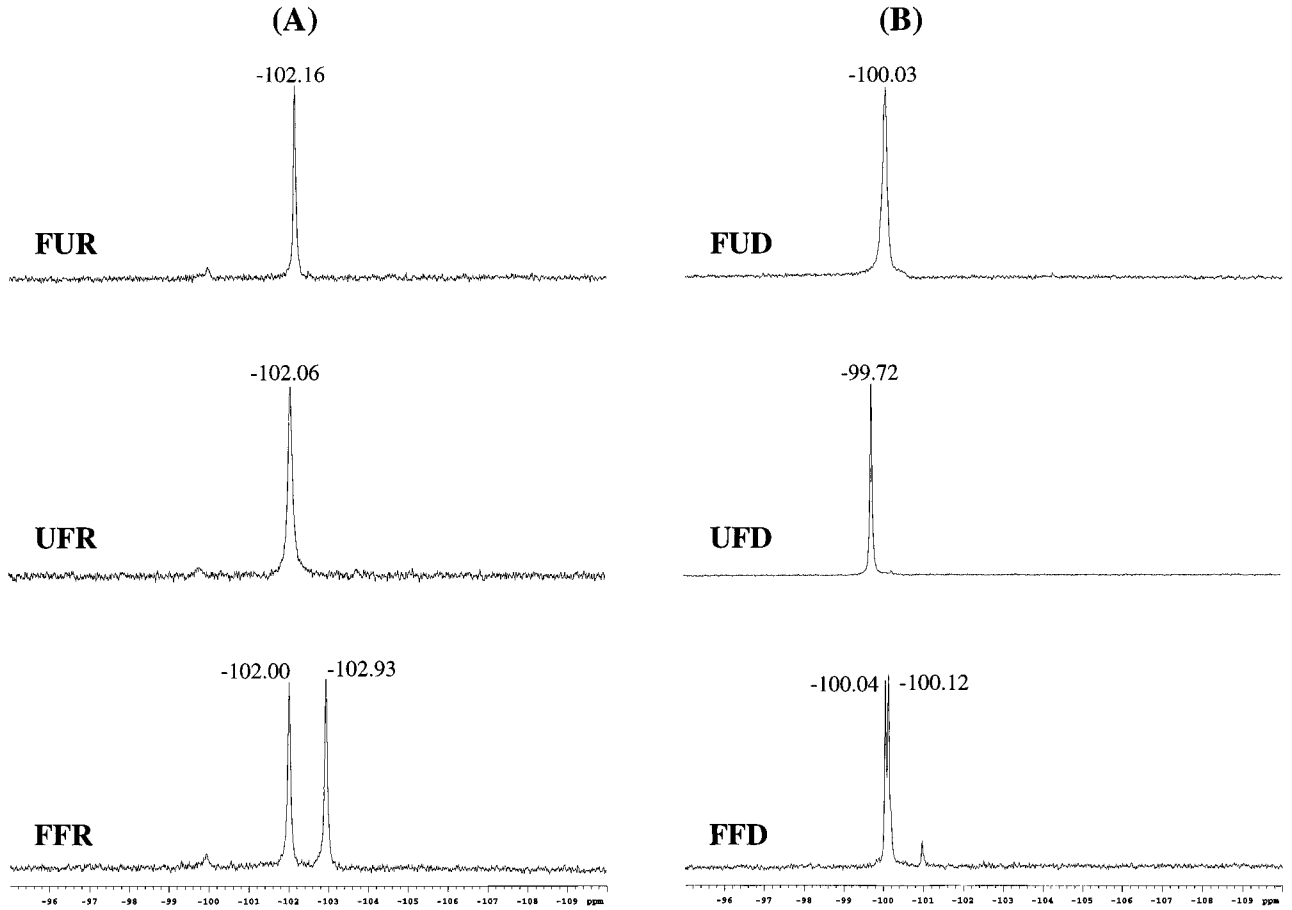

FIGURE 2: ^{19}F NMR spectra for the three RNA duplexes (A) and the three DNA duplexes (B) included in this study that contain FUrd or FdUrd. A single ^{19}F resonance is observed for the symmetrical duplexes substituted with FUrd/FdUrd at one site, and two ^{19}F resonances are observed for the doubly substituted duplexes.

downfield compared to their resonance values in dUrd (Urd) as a consequence of the electron-withdrawing effects of the ^{19}F nucleus bound to the adjacent carbon (Sylvia & Gerig, 1993). Smaller differences in chemical shift are observed for the H8 resonances of dA residues in dA-FdUrd (A-FUrd) base pairs that are shifted downfield by about 0.04 ppm compared to the resonance values in dA-dUrd (A-Urd) base pairs, indicating that the electron-withdrawing inductive effect of ^{19}F is transmitted through hydrogen bonds as well as through the π-electron system of the aromatic base.

^{19}F NMR spectra show one resonance from the single FUrd in [FUR] and [UFR] and two resonances from each of the two FUrd nucleosides in [FFR] (Figure 2). Similar results are observed for the DNA duplexes. Assignment of the FUrd residues in [FFR] and [FFD] using heteronuclear Overhauser effect experiments was not successful due to unfavorable correlation times for these duplexes. ^{19}F resonances were therefore assigned by assuming that the FUrd with a downfield ^{19}F chemical shift in the individually substituted duplexes was also more downfield in [FFR] and [FFD] (Figure 2).

Subtle changes in chemical shift are observed for the ^{19}F resonances in the double helices that contain two FdUrd (FUrd) substitutions compared to the monosubstituted duplexes. These subtle differences in chemical shift are consistent with changes in base stacking due to FdUrd (FUrd) substitution observed in the final refined structures for these duplexes (see below). The sequence of the DNA and RNA duplexes contains two nonequivalent sites, Urd_6 and Urd_7 (Figure 1). Urd_6 has A_5 as its 5′-neighbor and Urd_7 as its 3′-neighbor. The chemical shift of $FdUrd_6$ in [FFD] is 0.1 ppm upfield relative to [FUD] (−100.12 *vs* −100.03; see Figure 2). The upfield shift at $FUrd_6$ is greater for the bissubstituted RNA duplex, resonating 0.8 ppm upfield in [FFR] relative to [FUR] (−102.93 *vs* −102.16; Figure 2). This upfield shift is consistent with increased stacking between $FUrd_6$ and $FUrd_7$ in the refined structure for [FFR] compared to [FUR] (see below and Figure 7). Increased stacking at the pyrimidine−pyrimidine step in this sequence is not observed for the DNA duplexes substituted with FdUrd although slight changes are observed in the stacking at purine−pyrimidine steps in the DNA duplexes (Figures 7 and 8). Urd_7 has Urd_6 as its 5′-neighbor and C8 as its 3′-neighbor. The chemical shift of $FdUrd_7$ in [FFD] is moved 0.3 ppm upfield relative to [FUD] (−100.04 *vs* −99.72; Figure 2). No upfield shift occurs at this position for the bissubstituted RNA duplex in contrast to what is observed for the DNA duplexes (−102.00 *vs* −102.06; Figure 2). No increase in base stacking is observed between $FUrd_6$ and $FUrd_7$ in the refined structure for [FFR] compared to [UFR] (Figure 7). Changes in ^{1}H chemical shift for H5 of Urd_6 and Urd_7 in [UFR] and [FUR] compared to [UUR] also occur and are consistent with increased base stacking occurring between $FUrd_6$ and Urd_7 (Supporting Information and Figure 7).

Sugar Torsional Angles. Estimation of the torsional angles for the deoxyribose sugars was accomplished by comparing the cross peak fine structure from experimentally acquired

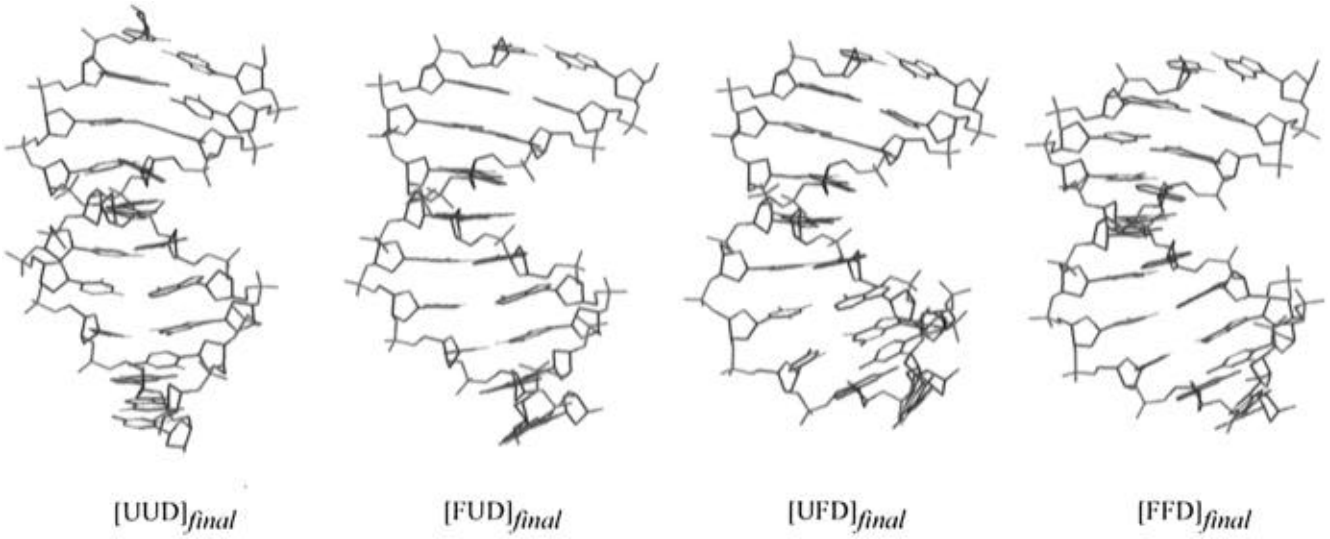

FIGURE 3: Final structures of the four DNA duplexes [UUD], [UFD], [FUD], and [FFD] as determined by restrained molecular dynamics simulations using the experimental distance and torsion angle constraints. The structure determination protocol is described in detail in the text.

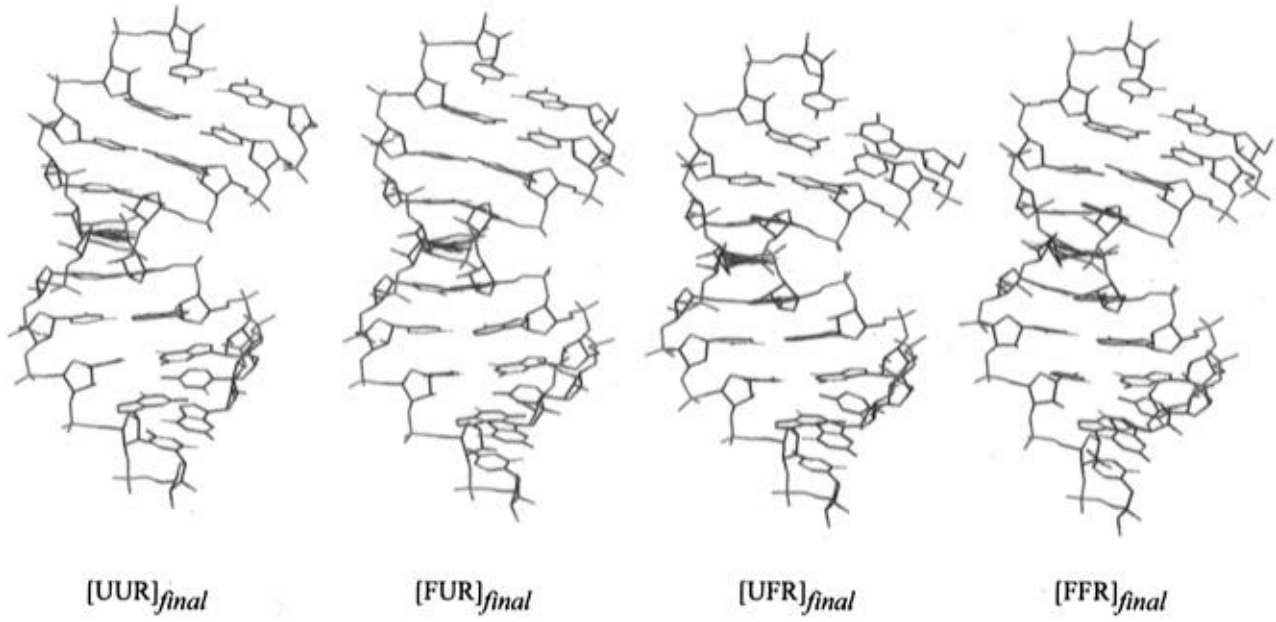

FIGURE 4: Final structures of the four RNA duplexes [UUR], [UFR], [FUR], and [FFR] as determined by restrained molecular dynamics simulations using the experimental distance and torsion angle constraints. The structure determination protocol is described in detail in the text.

DQCOSY spectra to simulated DQCOSY spectra that were generated with the programs SPHINX and LINSHA (Widmer & Wuthrich, 1987). Comparison of all of the simulated spectra with the experimental DQCOSY spectra did not identify a simulation within the range of parameters varied that uniquely matched the experimental data. Consequently, a dynamic two-state model with two rapidly interconverting sugar conformations (one from the S and one from the N region of the pseudorotation circle) was considered. The pseudorotation phase angles of the dominant S conformer, P_S, varied from 135° to 162° and the S population ranged from 75% to 95% for all of the deoxyribose sugars. The sugar pucker amplitude, $\phi_m{}^S$, was 37°. The parameters $P_N = 9°$ and $\phi_m{}^N = 37°$ were assumed for simulations of the minor conformer. The cross peak patterns from the DQCOSY spectra for FdUrd nucleosides in duplexes substituted with FdUrd were not significantly different from the dUrd nucleosides. The spectral simulation data are available as part of the Supporting Information.

The ribose sugars were estimated to have pseudorotation angles of 34°, and torsional angles were restrained to be near this value during the rMD simulations. This estimation of the pseudorotation angle for the ribose sugars is consistent with the CD spectra of the native and all three FUrd-substituted RNA duplexes that indicate adoption of A-form geometry by these duplexes (Sahasrabudhe *et al.*, 1995), by the presence of strong cross peaks for base proton to H1′ interactions in NOESY spectra for all nucleosides of all four RNA duplexes (and weaker intraresidue base proton to H2′ cross peaks in the same spectra), and by the absence of cross peaks for the H1′−H2′ interactions in the DQCOSY spectra for these same RNA duplexes. Based on the digital resolution of the DQCOSY spectra, the $^3J_{H1'-H2'}$ interaction is less than 3 Hz for all nucleosides, placing the pseudoro-

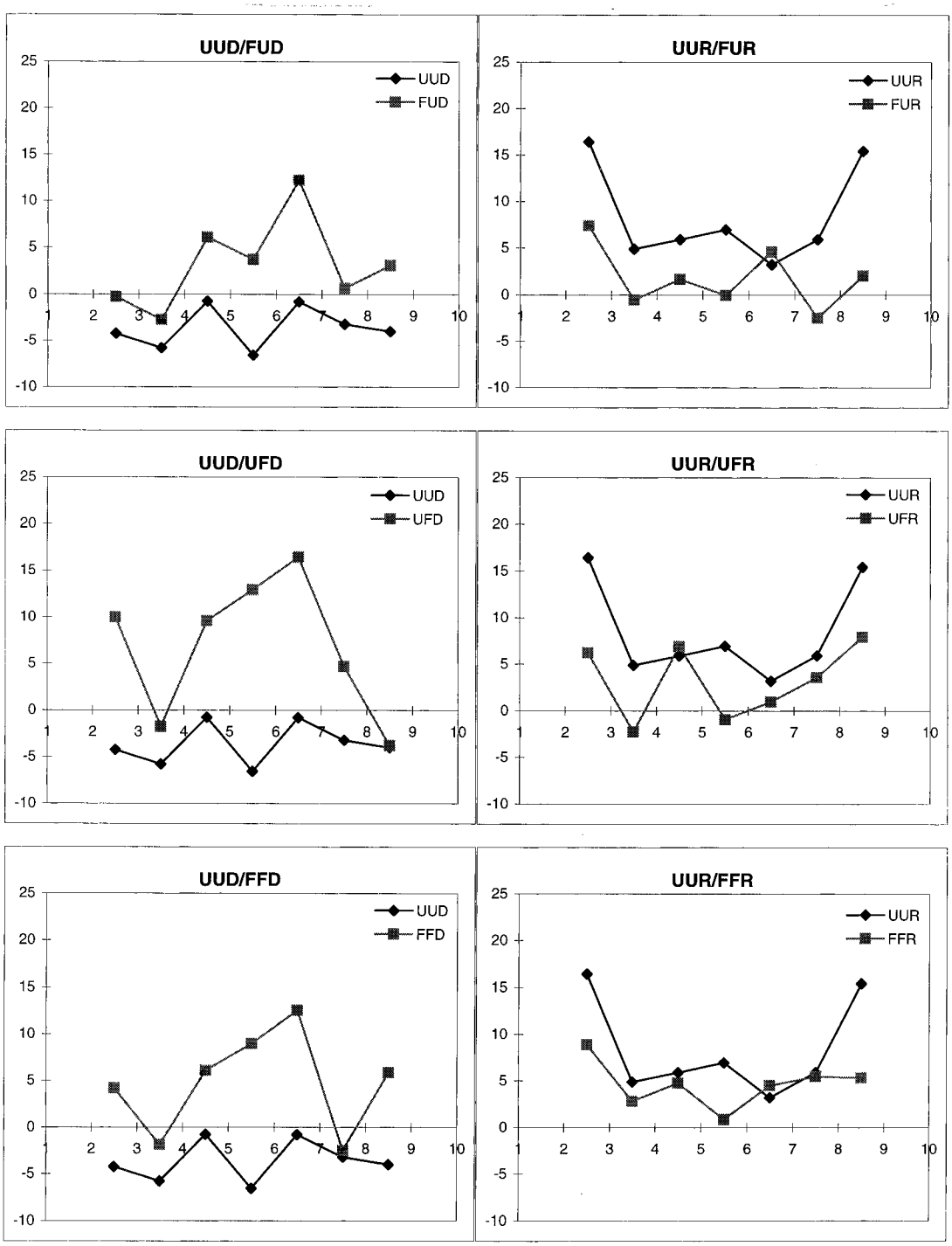

FIGURE 5: (A, left) Comparison of the helical parameter roll for the central A-U base pairs of the three DNA duplexes substituted with FdUrd ([FUD], [UFD], and [FFD]) compared to the control duplex [UUD]. (B, right) A similar comparison of the value of roll for the central A-U base pairs of the three RNA duplexes substituted with FUrd ([FUR], [UFR], and [FFR]) compared to the control duplex [UUR].

tation angle in the 26° to 40° range. The lack of resolvable fine structure in the DQCOSY spectra prevents the application of spectral simulation for determining sugar torsional angles. The similarities in the intensities for intraresidue base proton to H1′ and H2′ in the native and FUrd-substituted duplexes indicate that sugar conformation does not change significantly in the FUrd-substituted RNA duplexes, even for the residues directly substituted.

Effects of FdUrd Substitution on Duplex DNA. The final structures for [UUD], [UFD], [FUD], and [FFD] are shown in Figure 3. The final DNA structures are all clearly B-form helices, as is evident from the RMS deviations listed in Table 2. The effects of FdUrd substitution to the structure of duplex DNA were determined by conducting an analysis of 20 helical parameters (Dickerson, 1989) for each DNA duplex using the program DIALS and WINDOWS (Ravishanker *et al.*, 1989). The values for each of these helical parameters for the FdUrd-substituted DNA duplexes [FUD], [UFD], and [FFD] were compared to the control DNA duplex [UUD]. The model duplex chosen ([UUD] = (5′ dGCGAAUUCGC)$_2$) was selected so that FdUrd substitution would be near the center of the duplex and end-fraying of the duplex at terminal base pairs would not mask structural effects due to FdUrd substitution.

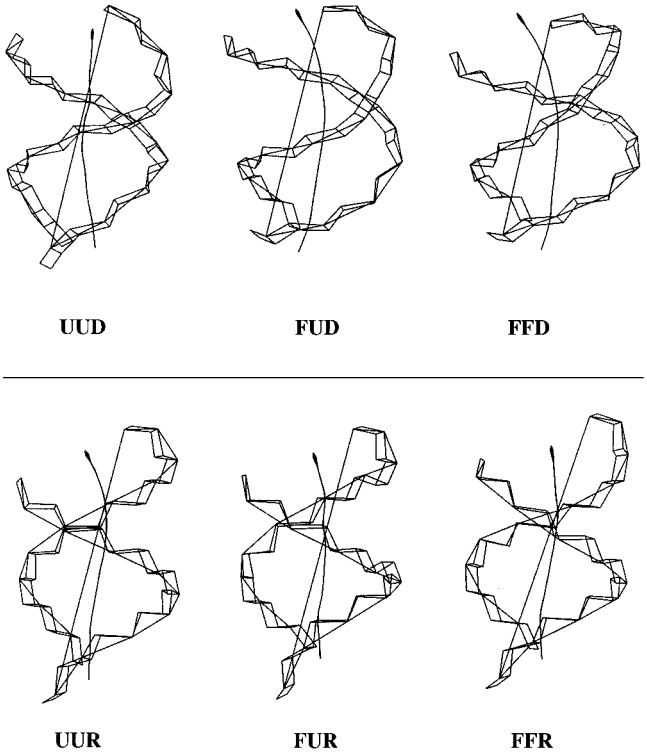

FIGURE 6: Depiction of the helical structure and the helical axis for the four DNA duplexes and the four RNA duplexes determined in the present study. The increased roll parameter for the FdUrd-substituted DNA duplexes results in bending of the helical axes. This bending is not observed for the RNA helices.

The largest and most systematic differences in helical parameters that arise from FdUrd substitution in DNA duplexes occur for the roll angle that measures the relative inclination of two consecutive base pairs toward the major groove. The roll angle is approximately 10° more positive when one or both of the dA-dUrd base pairs of the DNA duplexes are substituted by a dA-FdUrd base pair (Figure 5). This increase in roll angle observed at consecutive base pairs when an dA-dUrd base pair is substituted with a dA-FdUrd base pair causes the helical axis of FdUrd substituted duplexes to be bent compared to the control duplex (Figure 6). Curvature of the helical axis has been observed previously in DNA sequences with four or more consecutive dA-dT base pairs (Haran *et al.*, 1994; Goodsell & Dickerson, 1994).

The bending of the helical axis of FdUrd-substituted duplexes is consistent with differences in interproton distances that have been shown by others to be characteristic of DNA curvature. Such differences in interproton distances are manifest both in the volumes of cross peaks from NOESY data and in the distances obtained from the MARDIGRAS calculations that were used as constraints in the rMD simulations. Three types of distances were observed to systematically vary in DNA duplexes substituted with FdUrd compared to the control DNA duplex: (1) interresidue distances between H6 of $dUrd_6$, $dUrd_7$, or dC_8 and H1′, H2′, and H2′′ of the preceding residue (A_5, $dUrd_6$, or $dUrd_7$); (2) intraresidue distances between H6 and H1′, H2′, and H2′′ of $dUrd_6$ and $dUrd_7$; and (3) interresidue distances between H1′ and H2 ($dUrd_6$-A_5 and $dUrd_7$-A_4). The DNA duplexes with one FdUrd ([UFD] and [FUD]) showed similar changes for each type of distance compared to [UUD]. For [UFD] and [FUD] both the interresidue distances and the intraresidue distances between base protons and sugar protons were lengthened at the site of FdUrd substitution. These distances were not observed to lengthen for the dUrd site not substituted with FdUrd (except the interresidue distances to neighboring FdUrd). Bending of the helical axis for [UFD] and [FUD] relative to [UUD] arises from changes only involving distances at the site of FdUrd substitution and distances between FdUrd and its 5′ and 3′ neighbors.

Table 3: Pairwise RMS Deviations between the Control and FdUrd-Substituted DNA Oligonucleotides

base pair	UUD-FUD	UUD-UFD	UUD-FFD
C2-G19	1.275	2.013	2.367
G3-C18	0.995	1.709	1.707
A4-U/F17	1.067	1.543	1.585
A5-U/F16	1.080	1.590	1.843
U/F6-A15	1.106	1.688	1.718
U/F7-A14	1.053	1.886	1.492
C8-G13	1.059	1.944	1.893
G9-C12	1.118	2.482	2.314

Table 4: Pairwise RMS Deviations between the Control and FUrd-Substituted RNA Oligonucleotides

base pair	UUR-FUR	UUR-UFR	UUR-FFR
C2-G19	1.122	1.006	0.836
G3-C18	0.626	0.689	0.749
A4-U/F17	0.446	1.721	1.713
A5-U/F16	1.676	0.812	1.688
U/F6-A15	1.649	0.689	1.708
U/F7-A14	0.697	1.755	1.755
C8-G13	0.496	0.783	0.794
G9-C12	1.161	1.054	1.003

Changes in the three types of distances described above in relation to bending of the helical axis for [UFD] and [FUD] also occur in [FFD]. The changes observed for the bissubstituted duplex, however, differ from the monosubstituted cases in certain aspects. The intraresidue distances (type 2) behave similarly in the bissubstituted duplexes as for the monosubstituted duplexes in that they are lengthened for the FdUrd-substituted site. Similarly, the interresidue distances between H6 of $FdUrd_7$ and the sugar protons of $FdUrd_6$ are lengthened in the bissubstituted duplex relative to [UUD]. However, interresidue distances between H6 of C_8 and $FdUrd_6$ and the sugar protons of $FdUrd_7$ and A_5 are not lengthened in [FFD] even though these same distances are lengthened in [UFD] and [FUD]. The net result of the changes in distance observed for [FFD] is that the bending of the helical axis for the bissubstituted duplex [FFD] is about the same as for either of the monosubstituted duplexes [UFD] and [FUD] (∼10° for each). A summary of the changes in interresidue and intraresidue distances that are responsible for bending of the helical axis in FdUrd-substituted DNA duplexes is shown in Table 5.

Analysis of the remaining helical parameters for the four DNA duplexes did not reveal any other systematic differences in DNA structure that resulted from FdUrd substitution in duplex DNA that might be useful in correlating structural effects due to FdUrd substitution to the biological consequences of treatment with FUra. The values of helical parameters other than roll that measure rotations between two consecutive base pairs, e.g., twist and tilt, are unaffected by FdUrd substitution. Measures of the translations involving two consecutive base pairs (shift, slide, and rise) also did not vary upon substitution of FdUrd in a dA-dUrd base

Table 5: Some Interresidue and Intraresidue Distances from FdUrd-Containing DNA Oligonucleotides Compared with the Control[a]

distances	FUDNA	UFDNA	FFDNA
interresidue 5A−6U/FU	+	0	0/−
intraresidue 6U/FU	+	0	+
interresidue 6U/FU−7U/FU	+	+	+
intraresidue 7U/FU	0	+	+
interresidue 7U/FU−8C	0	+	0/−

[a] + indicates an increase, 0 indicates no change, and − indicates a decrease in the distance.

pair. Rotation angles for the dA and FdUrd bases of dA-FdUrd base pairs (opening, buckle, tip) were similar to those of dA-dUrd base pairs, except for the propeller twist that was decreased several degrees for the dA-FdUrd base pairs. Stagger between the dA and FdUrd bases of a dA-FdUrd base pair was somewhat attenuated from that found for the dA-dUrd base pair in the control, while other translations involving the dA-dUrd base pairs did not vary. The values for three helical parameters, shift, rise, and propeller twist, for the final structures of [UUD] and [UFD] are available as part of the Supporting Information.

The stacking of consecutive base pairs in the A-U rich center of the four DNA duplexes was analyzed to determine if FdUrd substitution affects base stacking in duplex DNA. Two base pair steps were analyzed for each of the four DNA duplexes. The first step involved the stacking of the A4-U17 and A5-U16 base pairs (Figure 7) while the second step involved stacking of the A5-U16 and the U6-A15 base pairs (Figure 8). The nomenclature for the base pairs in the DNA duplexes is given in Figure 1. The stacking pattern observed for the control and for each of the FdUrd-substituted duplexes is largely that expected from B-form duplex DNA (Schweitzer *et al.*, 1994). There is a high degree of intrastrand base overlap at the purine−pyrimidine steps but little intrastrand base overlap at pyrimidine−purine base steps. Intrastrand base overlap is minimal at purine−purine steps and essentially nonexistent at pyrimidine−pyrimidine steps. The effects of FdUrd substitution to helical stacking are greatest at purine−pyrimidine steps where FdUrd substitution augments the relatively large base stacking arrangement that is already present in the nonsubstituted duplex. Successive FdUrd substitutions, as occurs for [FFD], further increase the overlap of stacked bases at the purine−pyrimidine step. This increased overlap of stacked bases at purine−pyrimidine steps due to FdUrd substitution may be responsible for the enhanced stability observed previously for DNA duplexes substituted with FdUrd (Sahasrabudhe *et al.*, 1995).

Effects of FUrd Substitution on Duplex RNA. The final structures for [UUR], [UFR], [FUR], and [FFR] are shown in Figure 4. The effects of FUrd substitution to the structure of duplex RNA were analyzed by comparing the helical parameters for the FUrd-substituted duplexes [UFR], [FUR], and [FFR] to the control duplex [UUR]. The same 20 helical parameters were evaluated for the final RNA structures as were described for the DNA structures (Dickerson, 1989). One notable difference between the RNA sequences substituted with FUrd compared to the DNA sequences substituted with FdUrd is that the roll angle between consecutive base pairs is not affected by FUrd substitution in duplex RNA (Figure 5). The insensitivity of the roll angle in duplex RNA

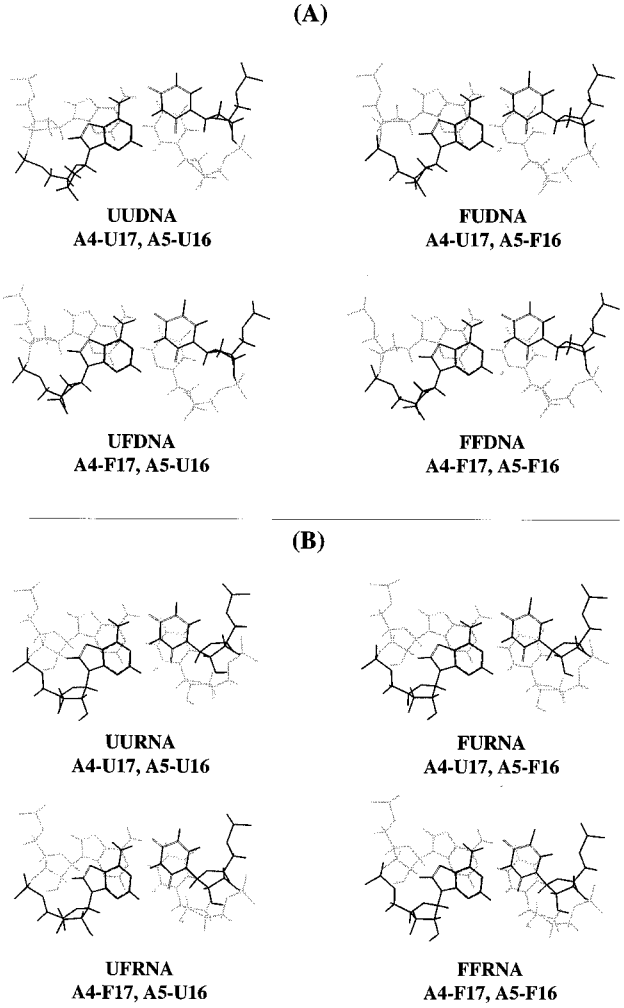

FIGURE 7: Representation of the base overlap that occurs at the purine−purine step between A4-U(F)17 and A5-U(F)16 base pairs for (A) the four DNA duplexes considered in the present study and (B) the four RNA duplexes. Base numbering is shown in Figure 1.

to substitution with FUrd results in the longitudinal (*z*) axis in the RNA duplexes substituted with FUrd being essentially unchanged from that of the control duplex (Figure 6). The values of other helical parameters also do not vary systematically with FUrd substitution. The values for shift, rise, and propeller twist for [UFR] and [UUR] along with the corresponding values of these parameters for [UFD] and [UUD] are available as part of the Supporting Information. The effects of FUrd substitution on base stacking in duplex RNA are similar to those observed in duplex DNA. FUrd substitution further augments the already substantial base stacking that occurs at purine−pyrimidine steps (Figure 8). This enhanced base stacking may be responsible for the greater stability of RNA duplexes substituted with FUrd compared to control duplexes (Sahasrabudhe *et al.*, 1995).

The structural effects most evident in FUrd-substituted duplexes compared to control duplexes are observed in a comparison of the RMS deviations for individual base pairs. The RMS deviations for A-Urd base pairs not substituted with FdUrd or for G-C base pairs in RNA duplexes substituted with FUrd are all less than 1.0 Å compared to the control RNA duplex. The RMS deviations for all A-FUrd base pairs are, in contrast, between 1.5−2.0 Å compared to the coordinates for the A-Urd base pairs in the control duplex (Table 3). No such systematic variation in

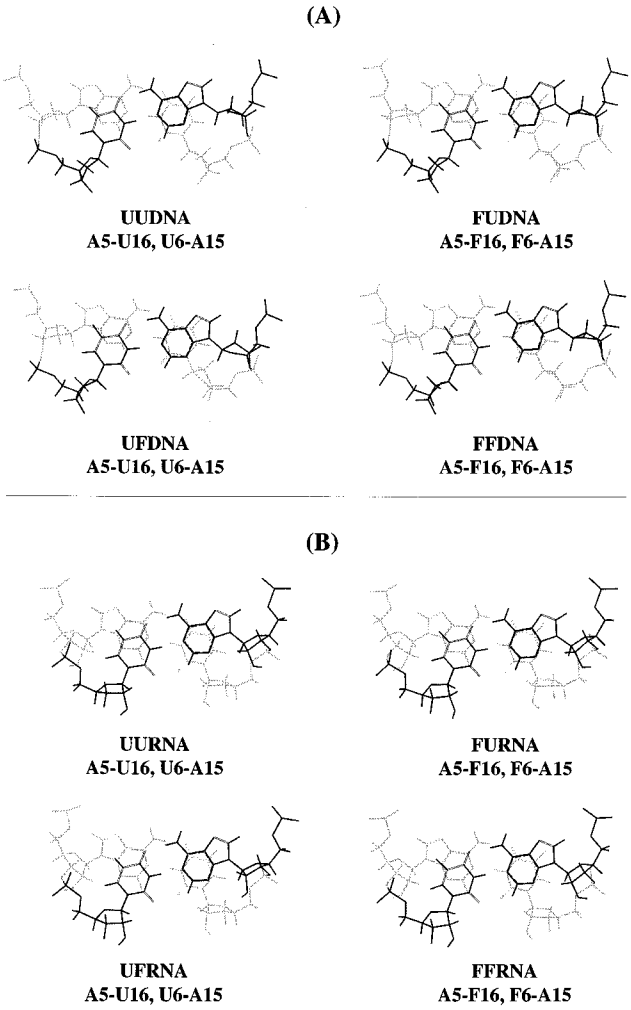

FIGURE 8: Representation of the base overlap that occurs at the purine−pyrimidine step between A5-U(F)16 and U(F)6-A15 base pairs for (A) the four DNA duplexes considered in the present study and (B) the four RNA duplexes. Base numbering is shown in Figure 1.

RMSD values for the dA-FdUrd base pairs of duplex DNA was observed (Table 2). This displacement of A-Urd base pairs upon FUrd substitution may impact the binding affinity for duplex RNA by proteins that bind duplex RNA. The altered affinity for duplex RNA by RNA-binding proteins may be responsible, in part, for the observed alterations in the processing of RNA in cells treated with FUra.

DISCUSSION

The anticancer drug FUra was first synthesized nearly 40 years ago, and combination chemotherapy including FUra is currently utilized in the treatment of most solid tumors, particularly for malignancies of the gastrointestinal tract, breast, head, and neck. FUra is an antimetabolite, and three products of its metabolic activation, FdUMP, FdUTP, and FUTP, are each considered responsible for part of its anticancer activity. FdUMP is a potent inhibitor of thymidylate synthase and is the metabolite responsible for the cytotoxicity of FUra in most instances. Deprivation of thymidine monophosphate due to FUra treatment is insufficient to induce cytotoxicity, at least in some instances, and incorporation of FdUTP into DNA and FUTP into RNA may be important for the cytotoxicity of FUra (Spiegelman *et al*., 1980). It is likely that the longstanding and widespread utility of FUra for the treatment of solid tumors results from the occurrence of multiple mechanisms of cytotoxicity for this drug.

The importance of FdUTP incorporation into genomic DNA for the activity of FUra is demonstrated by numerous reports indicating that DNA isolated from cells treated with FdUrd had undergone strand scission (Willmore & Durkacz, 1993). Resistance of a human ovarian cancer cell line to FUra has also been associated with decreased levels of FdUrd in DNA (Chu *et al*., 1990). A number of investigations into the structural properties of duplex DNA that contains FdUrd have been pursued in order to establish that the altered biological properties of FdUrd-containing genomic DNA are a consequence of altered structural characteristics that can be detected in relatively short duplex oligodeoxynucleotides. We report here that FdUrd substitution in DNA decamer duplexes affects the helical parameter roll at the nucleotide step of substitution and causes bending of the helical axis for FdUrd-substituted duplexes compared to duplexes that contain dUrd. While our results are in qualitative agreement with previous investigations describing the structures of duplex DNA containing FdUrd, the present study is unique in that direct comparison between the structures of the same DNA sequence with and without FdUrd substitution was made. Differences between the structure of the DNA sequence containing dUrd and the same sequence with a FdUrd substitution were observed that reveal FdUrd substitution is directly responsible for bending of the DNA-helical axis. Interestingly, substitution of two FdUrd in this sequence does not significantly increase the bend in the helical axis above that observed for the monosubstituted case. These results indicate that caution needs to be exercised in using FdUrd-substituted DNA duplexes to investigate the structure of nonsubstituted DNA (Rastinejad & Lu, 1993; Gmeiner *et al*., 1990).

The effects of FdUrd substitution in duplex DNA have been investigated previously using NMR spectroscopy and X-ray crystallography. Kremer and co-workers conducted NMR studies on the Pribnow recognition sequence and reported that FdUrd substitution destabilized the DNA duplex due to ionization of the FdUrd imino proton (Kremer *et al.*, 1987). The NMR spectroscopic studies of Sowers and co-workers on a 7-mer duplex containing a central dA-FdUrd base pair revealed that duplex DNA substituted with FdUrd adopts a normal right-handed configuration with a dA-FdUrd Watson−Crick base pair (Sowers *et al.*, 1987). In a separate study, Sowers and co-workers determined that a dG-FdUrd base pair alternates between a wobble and an ionized base pair as a function of pH (Sowers *et al.*, 1988). A dG-FdUrd wobble base pair was also observed in Z-form DNA in an X-ray crystallographic investigation (Coll *et al.*, 1989). Detailed analysis of the structure of a duplex octamer containing a single FdUrd revealed local conformational changes in the DNA helix that were attributed to FdUrd substitution (Stolarski *et al.*, 1992). In particular, the authors reported some irregularities in the helix axis that had a global curvature of 5.8° but with more pronounced bends near FdUrd-dA base pairs. The FdUrd-dA base pairs also had the smallest inclination and the largest tip angle observed in this structure. The structures of the DNA decamer duplexes determined in the present study reveal a systematic change in the roll angle for steps involving FdUrd-dA base pairs compared to dUrd-dA base pairs, in agreement with the

report of Stolarski *et al.* (1992). However, no systematic changes regarding inclination or tip angle were observed in the duplexes that are the subject of the present report that could be accounted for by FdUrd substitution. Effects of FdUrd substitution on tip angle and inclination may occur only in certain DNA sequences. Conversely, larger than average tip angles and inclination may also occur at this same position in the unsubstituted duplex studied by Stolarski *et al*., the structure of which was not reported. These differences between the structures reported in the present study and those reported previously demonstrate the advantage of comparing the structures of the same DNA sequence in the presence and absence of a modified base for understanding the structural effects that are caused by substitution.

The effects of FUrd substitution to the structure of duplex RNA are less well studied than the corresponding effects of FdUrd substitution in duplex DNA. FUrd substitution in duplex RNA stabilizes the RNA duplex, particularly for FUrd substitution at C-U mismatched base pairs and at A-U base pairs adjacent to G-U wobble base pairs (Sahasrabudhe *et al.*, in preparation). CD studies reveal that duplex RNA substituted with FUrd maintains an A-type helical geometry (Sahasrabudhe *et al.*, 1995). The greater variety of structures possible for RNA, e.g., stem−loops and pseudoknots, suggests that FUrd substitution in duplex RNA may not play a significant role in perturbing RNA-mediated processes. Structural effects have been observed for the U4 and U6 snRNPs isolated from murine sarcoma cells treated with FUra (Armstrong *et al.*, 1988). Nonetheless, duplex RNA structures play important roles in RNA-mediated processes, particularly as recognition sites for RNA-binding proteins.

The structures of the RNA decamer duplexes determined in the present study reveal that FUrd substitution affects the structures of RNA duplexes, although the effects are not large. The principal effect of FUrd substitution in RNA duplexes is increased base stacking at the site of FUrd substitution. Single FUrd substitutions in RNA duplexes are stabilizing (Sahasrabudhe *et al*., 1995), and the structures of the RNA duplexes determined in the present study strongly suggest that the increased thermal stability arises from greater base overlap. The increased roll angle observed in DNA decamer duplexes substituted with FdUrd does not occur in the RNA decamer duplexes, probably because the natural roll angle of the A-form duplex is large enough to accommodate distortion arising from changes in the preferred base stacking geometry of FUrd. No systematic change with regard to tip angle or inclination, as was observed previously in duplex DNA substituted with FdUrd, is observed in the RNA duplexes substituted with FUrd. Distortion in both RNA and DNA duplexes is limited to changes in the geometries of the site directly substituted with FUrd (FdUrd).

Evidence that nucleic acid mediated processes are altered by the incorporation of FUra metabolites into both DNA and RNA is both compelling and longstanding. The extent to which the perturbation of nucleic acid mediated processes is due to alteration of the structures of duplex RNA and DNA is not known, at present. The present study documents that substitution of FdUrd and FUrd into duplex DNA and RNA, respectively, results in a duplex of altered structure compared to the native duplex. These results suggest that the altered biological activity of nucleic acids substituted with FdUrd and FUrd may result from alterations in nucleic acid structure.

ACKNOWLEDGMENT

The authors thank Dr. Jack Horowitz for critical reading of the manuscript.

SUPPORTING INFORMATION AVAILABLE

Seven tables giving nonexchangeable ^{1}H chemical shifts from 5′-d and 5′-r GCGAAUUCGC and ^{19}F chemical shifts for the DNA and RNA oligonucleotides, chemical shifts for base H6/H8 and sugar H1′ protons for all four DNA and RNA oligonucleotides, energy terms and constraint deviations for the structures from RMD runs on DNA and RNA oligonucleotides, and comparison of crystallographic *R* factors and sixth root residual indices for starting model resulting RMD structures and three figures showing fingerprint regions from the 2D NOESY spectra, comparison of experimental and simulated DQCOSY spectra, and some helical parameters for UUD, UFD and UUR, UFR (10 pages). Ordering information is given on any current masthead page.

REFERENCES

Alderfer, J. L., Soni, S.-D., Arakali, A. V., & Wallace, J. C. (1993) *Photochem. Photobiol. 57*, 770−776.
Armstrong, R. D., Takimoto, C. H., & Cadman, E. C. (1986) *J. Biol. Chem. 261*, 21−24.
Arnott, S., & Hukins, D. W. L. (1972) *Biochem. Biophys. Res. Commun. 47*, 1504-1509.
Arnott, S., & Hukins, D. W. L. (1973) *J. Mol. Biol. 81*, 93-105.
Baleja, J. D., Pon, R. T., & Sykes, B. D. (1990) *Biochemistry 29*, 4828−4839.
Borgias, B. A., & James, T. L. (1988) *J. Magn. Reson. 79*, 493-512.
Borgias, B. A., & James, T. L. (1989) in *Methods in Enzymology, Nuclear Magnetic Resonance, Part A: Spectral Techniques and Dynamics* (Oppenheimer, N. J., & James, T. L., Eds.) Vol. 176, pp 169−183, Academic Press, New York.
Borgias, B. A., & James, T. L. (1990) *J. Magn. Reson. 87*, 475-487.
Chou, S.-H., Flynn, P., & Reid, B. (1989) *Biochemistry 28*, 2422−2435.
Chu, E., Lai, G.-I., Zinn, S., & Allegra, C. J. (1990) *Mol. Pharmacol. 38*, 410−417.
Clore, G. M., Oschkinat, H., McLaughlin, L. W., Benseler, F., Happ, C. S., Happ, E., & Gronenborn, A. M. (1988) *Biochemistry 27*, 4185−4197.
Coll, M., Saal, D., Frederick, C. A., Aymami, J., Rich, A., & Wang, H.-J. (1989) *Nucleic Acids Res. 17*, 911−923.
Dickerson, R. E. (1989) *Nucleic Acids Res. 17*, 1797−1803.
Dolnick, B. J., & Pink, J. J. (1985) *J. Biol. Chem. 260*, 3006−3014.
Doong, S.-L., & Dolnick, B. J. (1988) *J. Biol. Chem. 263*, 4467−4473.
Feigon, J., Leupin, W., Denny, W. A., & Kearns, D. R. (1983) *Biochemistry 22*, 5943−5951.
Gmeiner, W. H., Pon, R. T., & Lown, J. W. (1991) *J. Org. Chem. 56*, 3602−3608.
Gmeiner, W. H., Anderson, J., & Sahasrabudhe, P. (1994a) *Nucleosides Nucleotides 13*, 2329−2344.
Gmeiner, W. H., Sahasrabudhe, P., & Pon, R. T. (1994b) *J. Org. Chem. 59*, 5779−5783.
Gochin, M., & James, T. L. (1990) *Biochemistry 29*, 11172−11180.
Goodsell, D. S., & Dickerson, R. E. (1994) *Nucleic Acids Res. 22*, 5497−5503.
Gronenborn A. M., & Clore, G. M. (1989) *Biochemistry 28*, 5978−5984.
Haran, T. E., Kahn, J. D., Crothers, D. M. (1994) *J. Mol. Biol. 244*, 135−143.
Hare, D. R., Wemmer, D. E., Chou, S.-H., Drobny, G., & Reid, B. R. (1983) *J. Mol. Biol. 171*, 319−336.

Harris, D. R., & Macintyre, W. M. (1964) *Biophys. J. 4*, 203−225.
Hore, P. J. (1989) in *Methods in Enzymology, Nuclear Magnetic Resonance, Part A: Spectral Techniques and Dynamics* (Oppenheimer, N. J., & James, T. L., Eds.) Vol. 176, pp 216−241, Academic Press, New York.
James, T. L. (1991) *Curr. Opin. Struct. Biol. 1*, 1042−1053.
Kerwood, D. J., Zon, G., & James, T. L. (1991) *Eur. J. Biochem. 197*, 583−595.
Kim, J. K., Soni, S.-D., Arakali, A. V., Wallace, J. C., & Alderfer, J. L. (1995) *Nucleic Acids Res. 23*, 1810−1815.
Kremer, A. B., Mikita, T., & Beardsley, G. P. (1987) *Biochemistry 26*, 391−397.
Lavery, R., & Sklenar, H. (1988) *J. Biomol. Struct. Dyn. 6*, 63−91.
Lawrence, T. S., Davis, M. A., & Maybaum, J. (1994) *Int. J. Radiat. Oncol. 29*, 519−523.
Lee, M., Hartley, J. A., Pon, R. T., Krowicki, K., & Lown, J. W. (1988) *Nucleic Acids Res. 16 (2)*, 665−684.
Marion, D., & Wuthrich, K. (1983) *Biochem. Biophys. Res. Commun. 113*, 967−974.
Matsuoka, H., Ueo, H., Sugimachi, K., & Akiyoshi, T. (1992) *Cancer Invest. 10*, 265−269.
Mujeeb, A., Kerwin, S. M., Kenyon, G. L., & James, T. L. (1993) *Biochemistry 32*, 13419−13431.
Pearlman, D. A., Case, D. A., Caldwell, J. W., Ross, W. S., Cheatham, T. E., III, Ferguson, D. M., Seibel, G. L., Singh, U. C., Weiner, P., & Kollman, P. A. (1995) *AMBER 4.1*.
Pratt, W. B., Ruddon, R. W., Ensminger, W. D., & Maybaum, J. (1994) *The Anticancer Drugs*, 2nd ed., Oxford University Press, New York.
Rastinejad, F., & Lu, P. (1993) *J. Mol. Biol. 232*, 105−122.
Ravishanker, G., Swaminathan, S., Beveridge, D. L., Lavery, R., & Sklenar, H. (1989) *J. Biomol. Struct. Dyn. 6*, 669−699.
Rinkel, L. J., & Altona, C. (1987) *J. Biomol. Struct. Dyn. 4*, 621-649.
Ryckaert, J. P., Cicotti, G., & Berendsen, H. J. C. (1977) *J. Comput. Phys. 23*, 327-341.
Sahasrabudhe, P. V., Pon, R. T., & Gmeiner, W. H. (1995) *Nucleic Acids Res. 23*, 3916−3921.
Santi, D. V., McHenry, C. S., & Sommer, H. (1974) *Biochemistry 13*, 471−480.
Schmittgen, T. D., Danenberg, K. D., Horikoshi, T., Lenz, H.-J., & Danenberg, P. V. (1994) *J. Biol. Chem. 269*, 16269−16275.
Schmitz, U., Pearlman, D. A., & James, T. L. (1991) *J. Mol. Biol. 221*, 271−292.
Schmitz, U., Sethson, I., Egan, W., & James, T. L. (1992) *J. Mol. Biol. 227*, 510−531.
Schweitzer, B. I., Mikita, T., Kellog, G. W., Gardner, K. H., & Beardsley, G. P. (1994) *Biochemistry 33*, 11460−11461.
Singh, U. C., Weiner, P. K., & Kollman, P. A. (1985) *Proc. Natl. Acad. Sci. U.S.A. 82*, 755-759.
Sowers, L. C., Eritja, R., Kaplan, B. E., Goodman, M. F., & Fazakerley, G. V. (1987) *J. Biol. Chem. 262*, 15436−15442.
Sowers, L. C., Eritja, R., Kaplan, B. E., Goodman, M. F., & Fazakerley, G. V. (1988) *J. Biol. Chem. 263*, 14794−14801.
Spiegelman, S., Nayak, R., Sawyer, R., Stolfi, R., & Martin, D. (1980) *Cancer (Philadelphia) 45*, 1129−1134.
States, D. J., Haberkorn, R. A., & Ruben, D. J. (1982) *J. Magn. Reson. 48*, 286−292.
Stolarski, R., Egan, W., & James, T. L. (1992) *Biochemistry 31*, 7027−7042.
Suzuki, E., Pattabiraman, N., Zon, G., & James, T. L. (1986) *Biochemistry 25*, 6854-6865.
Sylvia, L. A., & Gerig, J. T. (1993) *Biochim. Biophys. Acta 1163*, 321−334.
Thomas, P. D., Basus, V. J., & James, T. L. (1991) *Proc. Natl. Acad. Sci. U.S.A. 88*, 1237−1241.
Weckbecker, G. (1991) *Pharmacol. Ther. 50*, 367−424.
Widmer, H., & Wuthrich, K. (1987) *J. Magn. Reson. 74*, 316-336.
Willmore, E., & Durkacz, B. W. (1993) *Biochem. Pharmacol. 46*, 205−211.
Yu, H., Eritja, R., Bloom, L. B., & Goodman, M. F. (1993) *J. Biol. Chem. 268*, 15935−15943.

BI960535Y